Cancer Cell International

RESEARCH Open Access

Organoids as a model system for researching human neuroendocrine tumor of the breast

Dongyi Zhao[1†], Xue Bai[1†], Shida Zhu[1†], Zuowei Zhao[1*] and Xuelu Li[1*]

Abstract

Background Neuroendocrine tumors primarily consist of endocrine cells commonly located in neural tissue and the endocrine system. Primary neuroendocrine neoplasms of the breast are highly heterogeneous tumors characterized by a diverse cell population. Their rarity in the breast poses considerable challenges in studying their pathogenesis and developing effective treatments.

Methods The surgical specimen was obtained from a Chinese female patient diagnosed with neuroendocrine tumor of the breast (NETB). We performed tissue histological staining and established NETB patient-derived organoids, which were subsequently used for histological staining, drug screen, and Single-cell RNA sequencing.

Results We successfully established NETB patient-derived organoids from a Chinese female patient. Histological staining showed that the morphological characteristics and the expression of molecular biomarkers (ER, PR, HER2, Ki67, Syn, CgA) in the NETB patient-derived organoids resembled those of the original tumor tissue. The NETB patient-derived organoids exhibited varying sensitivities to seven different drugs. Single-cell RNA sequencing revealed significant heterogeneity and diverse molecular functions among these organoids.

Conclusions This was the first instance of establishing an organoid model for NETB. Due to high heterogeneity, this NETB patient-derived organoid provides a robust foundation for clinical research. In the future, it could serve as a reliable tool for disease pathology diagnosis, drug screening, and genetic level studies.

Keywords Neuroendocrine neoplasms of the breast, Organoids, Histological staining, Drug screen, Single-cell RNA sequencing

Introduction

Neuroendocrine neoplasms of the breast, according to the recent fifth edition of the World Health Organization (WHO) classification, are subdivided into well-differentiated neuroendocrine tumor of the breast (NETB) and poorly differentiated neuroendocrine carcinoma of the breast [1]. Based on the morphology of the tumor cells, neuroendocrine carcinoma can be divided into small-cell neuroendocrine carcinoma and large-cell neuroendocrine carcinoma [1]. It has also been proposed that the diagnosis of neuroendocrine tumor or neuroendocrine carcinoma is appropriate only when the neuroendocrine tumor component constitutes more than 90% of the

†Dongyi Zhao, Xue Bai and Shida Zhu contributed equally to this work.

*Correspondence:
Zuowei Zhao
dmuzhaozuowei@163.com
Xuelu Li
dmulixl@163.com
[1]Department of Breast Surgery, The Second Hospital of Dalian Medical University, Dalian 116023, China

tumor, taking into account factors such as tumor differentiation, morphological characteristics, and other relevant criteria [1–3]. Neuroendocrine tumor is primarily composed of endocrine cells, commonly found in neural tissue and the endocrine system [4]. In clinical practice, the most common sites of occurrence are the lungs and the gastrointestinal tract [4]. Nevertheless, neuroendocrine neoplasms of the breast are relatively rare tumor, accounting for only 2%~5% of all women breast cancers [5, 6]. It is noteworthy that neuroendocrine differentiation is relatively common in invasive breast cancer, presenting in 10–30% of cases [7]. Primary neuroendocrine neoplasms of the breast are highly heterogeneous tumors composed of a diverse cell population [8]. Furthermore, the low incidence of neuroendocrine neoplasms of the breast makes studying their pathogenesis and treatment particularly challenging. Currently, there are no standard treatment options for these patients, and the prognosis for neuroendocrine neoplasms of the breast remains controversial. Only a few case reports or small retrospective series are available, and the experimental validation remains limited. Therefore, there is an urgent need for a precise model to facilitate further research on neuroendocrine neoplasms of the breast.

The organoid model is a miniature organ created in vitro from a small amount of fresh cancer tissue. This three-dimensional (3D) organoid closely resembles its in vivo counterpart [9, 10]. Organoid-based models of cancer are emerging as valuable platforms for cancer diagnosis, prognosis and treatment. Compared with animal models, the patient-derived organoids eliminate the variables introduced by animals and offer the advantage of personalization [11–13]. The low incidence of rare diseases, along with ethical issues, has posed significant challenges in research and resulted in a lack of precise treatment options for many of these conditions. The emergence of organoids has effectively addressed these challenges.

Materials and methods

Sample collection

The tumor specimen was obtained from the NETB patient during surgery. Within 10 min of being removed from the human body, the surgical tissue of NETB was placed in 5 ml cold AdDF+++ medium and was transferred to the laboratory within 15 min to begin processing. The fresh breast cancer tissue was cut into two pieces. A part of the tissue was fixed in formalin for immunohistochemistry. Another part of the tissue was used for organoid culture. This study was approved by the ethical committees of the Second Hospital of Dalian Medical University (Dalian, China). All the procedures were carried out in accordance with the Declaration of Helsinki.

Organoid culture

Sachs's protocol with minor modifications was used for organoid establishment [9].The fresh breast cancer tissue was cut into 1–2 mm^3 pieces, then washed with 1 ml of AdDF+++ medium in the 60-mm dish. The 1.5 mg/ml collagenase solution (Sigma, Saint Louis, MO, USA) about 1.5 ml was added to the dish to immerse the tissue, and incubated at 37℃ for 2 h. During incubation for collagenase digestion, the solution was mixed by gently pipetting a few times every 15–20 min. The digested tissue was collected in 3 ml AdDF+++, then centrifuged at 1500 rpm for 5 min. After discarding the liquid above, the tissue pellets were suspended in a mixture of 20 µl matrigel (Corning Incorporated, NY, USA) and 20 µl medium in a 24-well suspension plate (Corning Incorporated, NY, USA) at 37℃ for 20 min. When the matrigel was solidified, 400 µl of the medium was added to each well. The specific composition of the medium can be found in the referenced article [9, 14, 15]. The medium was changed every 3 days and pellets were typically passaged (1:2) every 2 ~ 3 weeks following size and morphology assessment. The protocol for 2D cultures is similar to that for 3D cultures: Tumor tissues were digested and centrifuged as previously described. After removing the supernatant, the cell suspension was seeded in a 24-well plate and supplemented with culture medium to a final volume of 400 µL.

Immunohistochemistry

For immunohistochemistry, NETB patient-derived organoids along with the culture supernatant were collected from the 24-well suspension plates completely, and centrifuged for 5 min at 1500 rpm. After discarding the supernatant, NETB patient-derived organoids pellets were embedded in HistoGel (Thermo Fisher Scientific, Waltham, Massachusetts) and solidified at 4℃ for 5 min. This final mixture and surgical specimen samples were fixed in 4% paraformaldehyde before being embedded in paraffin. After fixation, routine paraffin embedding would be produced and sliced up. The immunohistochemical method was applied to stain NETB patient-derived organoids and tissue sections according to the manufacturer instructions of a SP method kit and a DAB chromogenic kit (Zhongshan Golden Bridge Company, Beijing, China). The sodium citrate solution was used in antigen retrieval by microwave heating at 95 °C for 20 min. Slides were stained with primary antibody at 4 °C overnight. The primary antibodies illustrations were as follows: Anti-estrogen receptor alpha antibody (1:50, ab16660, Abcam), anti-progesterone receptor antibody (1:100, ab63605, Abcam), anti-ErbB2/HER2 antibody(1:1000, ab134182, Abcam), anti-Ki67 antibody(1:200, ab16667, Abcam) were purchased from Abcam (Cambridge, MA, UK). Anti-Syn antibody working fluid (ZM-0246) was

purchased from Zhongshan Golden Bridge Biotechnology Company (Beijing, China). Anti-CgA antibody working fluid was purchased from Maixin Company (Fuzhou, China).

Drug screen

The NETB patient-derived organoids of the fifth passage were digested and dissociated into single cells. After growing for 5 days, small size organoids were collected and diluted to 70 organoids/μl with medium containing 5% Matrigel. A 384-well plate (Nest, Wuxi, Jiangsu, China) was coated with 10 μl Matrigel, and was added to 30 μl organoids suspension. Then, 7 concentrations (0, 0.1μM, 1μM, 10μM, 20μM, 50μM, 100μM) of drugs were added, such as Tamoxifen, Fulvestrant, Palbociclib, Epirubicin, Carboplatin, Cisplatin, and Docetaxel. All of drugs above were obtained from MedChemExpress (MCE, Monmouth Junction, NJ, USA). After 5 days, 25 μl of CellTiter-Glo3D reagent (Promega, Madison, WI, USA) was added to each well. After 30 min of incubation at 20–25℃, the plate was read on a SpectraMax microplate reader. The experiments were independently repeated three times and each time had three replicates. The final data was analyzed using GraphPad Prism 6 and the IC50 values were determined.

Single-cell RNA sequencing

The NETB patient-derived organoids of the seventh generation were digested into single cells. Then, the cells in suspension were captured by microfluidic chips (Singleron Biotechnologies, Jiangsu, China). The genetic material from the cells was extracted and amplified to construct the libraries. After passing quality control, these libraries were sequenced (Illumina) according to the effective concentration and target data volume requirements. Raw reads were processed to generate gene expression profiles using the CeleScope v1.5.2 (Singleron Biotechnologies, Jiangsu, China) pipeline. Scanpy v1.8.2 was used for quality control, dimensionality reduction and clusterin [16]. The identity of each cell group is determined through the SynEcoSys database (Singleron Biotechnologies, Jiangsu, China). Cell differentiation trajectory was reconstructed with the Monocle2 [17]. Gene Ontology (GO) and Kyoto Encyclopedia of Genes and Genomes (KEGG) analysis were used with the "clusterProfiler" R package [18]. Finally, protein-protein interaction network analysis sourced from the STRING protein interaction database [19]. The libraries were generated and subjected to Single-cell RNA sequencing by a sequencing company (Singleron Biotechnologies, Jiangsu, China).

Results

Case report

A 36-year-old female patient initially discovered a bean-sized mass with notable nipple retraction about one month ago. The mass was hard, mobile, and non-tender, and no associated nipple discharge or pain. No treatment had been undertaken prior to her hospital admission. This patient reported no family history of cancer. The breast Magnetic Resonance Imaging (MRI) revealed a mass located behind the nipple, measuring approximately 3.5×3.4 centimeters. The mass was irregularly shaped and had invaded the nipple, causing its retraction (Fig. 1A). The MRI revealed that the mass invaded the skin of the affected breast, with mild surrounding edema (Fig. 1A). The mass exhibited heterogeneous enhancement, with a fluid-filled area measuring approximately 1.5×1.0 centimeters (Fig. 1B).

A core needle biopsy of the left breast tumor revealed NETB with small cell and focal spindle cell features. Subsequently, the patient underwent right breast conserving surgery without preserving the nipple-areola complex, along with axillary lymph node dissection. It was observed that the tumor was solid near the nipple and mucinous near the pectoral muscle, which was consistent with the preoperative breast MRI findings (Fig. 1C). Postoperative pathology revealed a tumor measuring 3.0×2.0×2.0 centimeters, along with a translucent and gelatinous mass measuring 2.0×1.0×1.0 centimeters, consistent with the diagnosis of NETB. The tumor invaded the dermal papillary layer. Out of the five sentinel lymph nodes, one exhibited metastasis. Immunohistochemical analysis revealed that hormone receptors were positive (90% estrogen receptors, 90% progesterone receptors), with the Ki67 index of 30%. The postoperative wound was healing well (Fig. 1D). Following surgery, the patient received systemic chemotherapy (epirubicin and cyclophosphamide followed by paclitaxel liposomes) and adjuvant radiotherapy. Additionally, the patient was treated with Goserelin and Letrozole.

Establishing NETB patient-derived organoids

Samples was taken from the fresh breast NETB specimen, and tumor tissue was treated as described in the Materials and Methods (Fig. 1C). The procedure was used to culture patient-derived organoids from the NETB. To distinguish differences between patient-derived organoids and 2D cells, we examined two different culture conditions separately. The 3D NETB patient-derived organoids were successfully established (Fig. 1C), while the 2D tumor cell culture was unsuccessful (Fig. 1C). The morphology of NETB patient-derived organoids was maintained after eight months of culture, with a similar growth rate observed throughout this period (Supplement Fig. 1). The NETB patient-derived organoids were

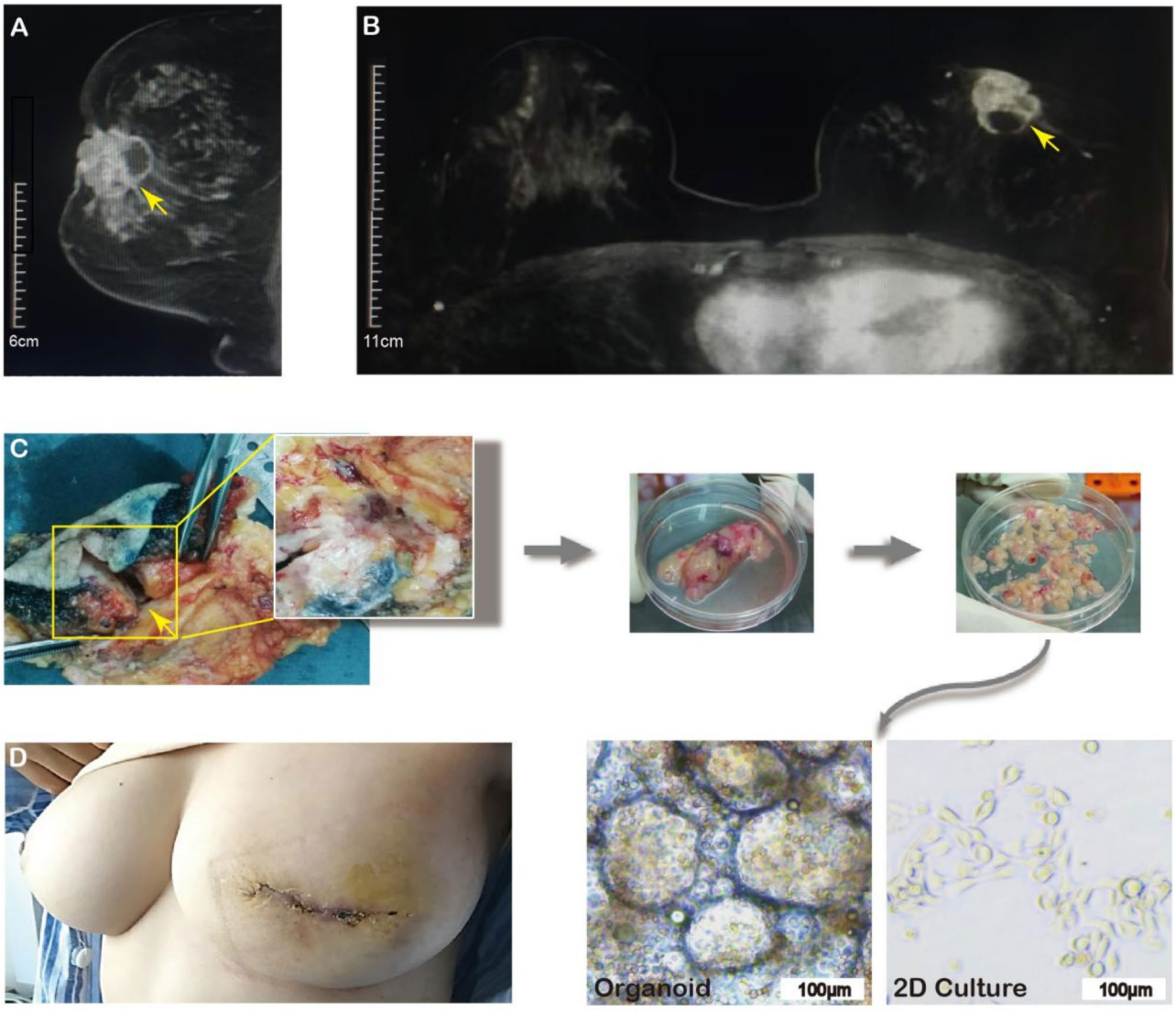

Fig. 1 Establishing NETB patient-derived organoids. **(A)** The breast MRI revealed a mass situated behind the nipple. The arrow indicates the cystic-solid mixed boundary of the tumor. **(B)** The breast MRI revealed that the mass exhibited heterogeneous enhancement, with a fluid-filled area. The arrow indicates the cystic-solid mixed boundary of the tumor. **(C)** During surgery, the tumor specimen was dissected, revealing the solid near the nipple and mucinous near the pectoral muscle. The tumor was cut into small pieces, digested, and then cultured. Representative images of the NETB patient-derived organoids and 2D culture. **(D)** The patient recovered well after the right breast-conserving surgery without preserving the nipple-areola complex, along with axillary lymph node dissection

successfully resuscitated and survived without any apparent loss of viability (Supplement Fig. 1). We successfully established NETB patient-derived organoids, which have been cultured for more than eight months.

The NETB patient-derived organoids maintained the characteristics of the original tumor tissue

To observe the structure of the NETB patient-derived organoids, the original tumor tissue and NETB patient-derived organoids were stained with hematoxylin and eosin (H&E). Immunohistochemistry was performed to examine the status of estrogen receptor (ER), progesterone receptor (PR), human epidermal growth factor receptor 2 (HER2), Ki67, synaptophysin (Syn), and Chromogranin A (CgA) status. Syn and CgA are markers used to diagnose NETB. The results showed that, in addition to breast cancer markers, the expression of Syn and CgA was preserved in NETB patient-derived organoids (Fig. 2). After a freeze-thaw process, these organoids could maintain the structure and molecular expression of the tumor tissue. However, after several passages, both ER/PR expression intensity and the proportion of

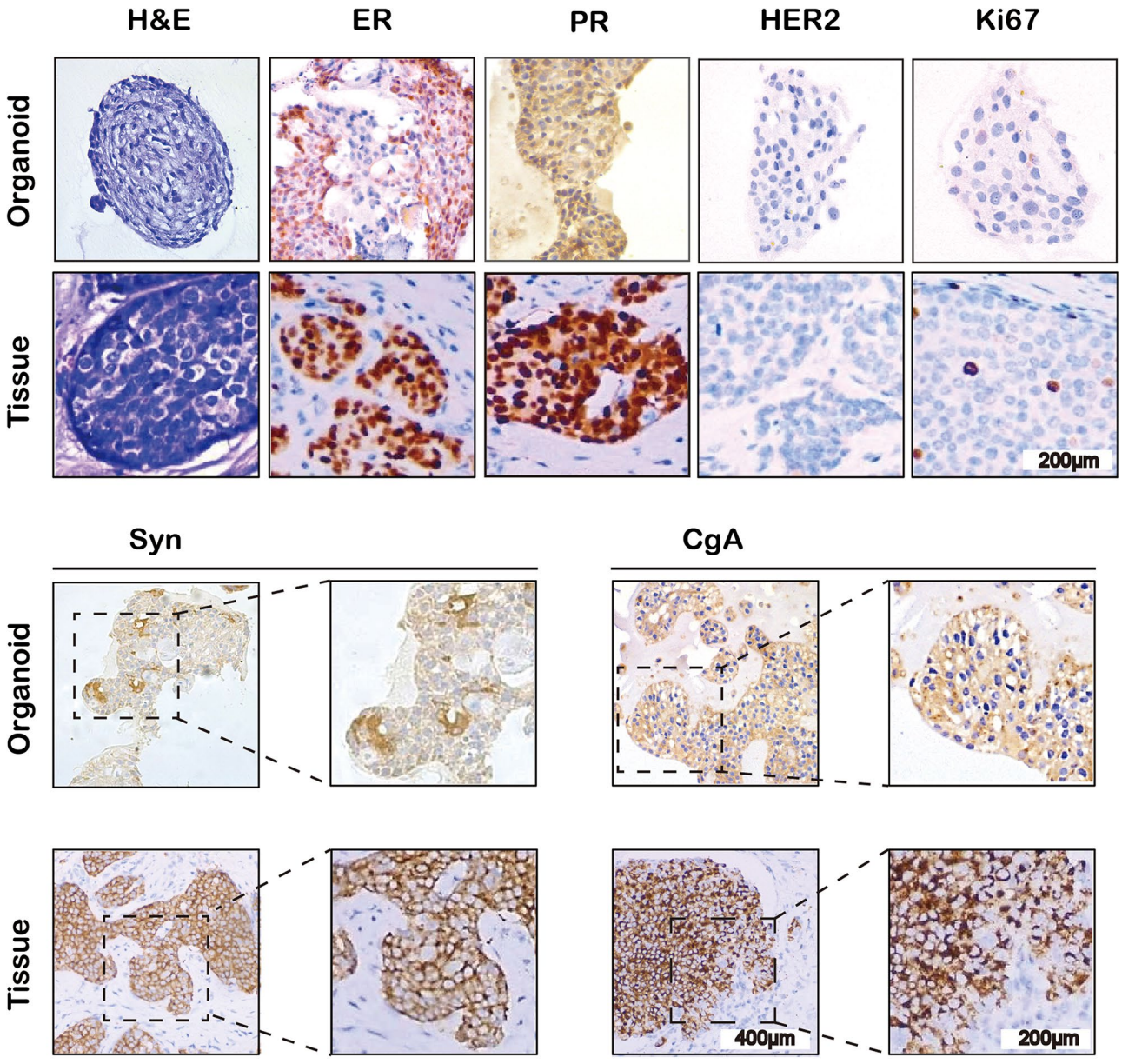

Fig. 2 The NETB patient-derived organoids retained the characteristics of the original tumor tissue. Representative images of hematoxylin and eosin (H&E) and immunohistochemistry staining (ER, PR, HER2, Ki67, Syn, CgA) of the NETB patient-derived organoids and the original tumor tissue. Estrogen receptor (ER), Progesterone receptor (PR), Human epidermal growth factor receptor 2 (HER2), synaptophysin (Syn), Chromogranin A (CgA)

positive cells were gradually reduced. Meanwhile, the proportion of Ki67 and HER2 positive cells increased somewhat (Fig. 3). Taken together, these results indicated that the histological features and molecular phenotypes of the NETB patient-derived organoids were similar but not an exact match to the original tumor tissue (Figs. 2 and 3).

The NETB patient-derived organoids provide potential strategies for clinical treatment

Drug testing was performed under 3D condition to mimic the in vivo condition. Among the seven drugs tested, the NETB patient-derived organoids showed the highest sensitivity to Epirubicin (IC50=0.1900μmol/L, 95% CI 0.1243 to 0.2905), and the lowest sensitivity to Carboplatin (IC50=28.71μmol/L, 95% CI 23.86 to 34.54). The susceptibility testing results were shown (Fig. 4), including Palbociclib (IC50=0.2786μmol/L, 95% *CI* 0.1643 to 0.4722), Docetaxel (IC50=0.4487μmol/L, 95% *CI* 0.3244 to 0.6206), Tamoxifen (IC50=1.111μmol/L, 95% *CI* 0.9173 to 1.345), Cisplatin (IC50=1.27μmol/L, 95% *CI* 0.6185 to 2.625), and Fulvstrant (IC50=2.104μmol/L, 95% *CI* 0.9865 to 4.488). Indeed, the NETB patient-derived organoids exhibited various sensitivities to the

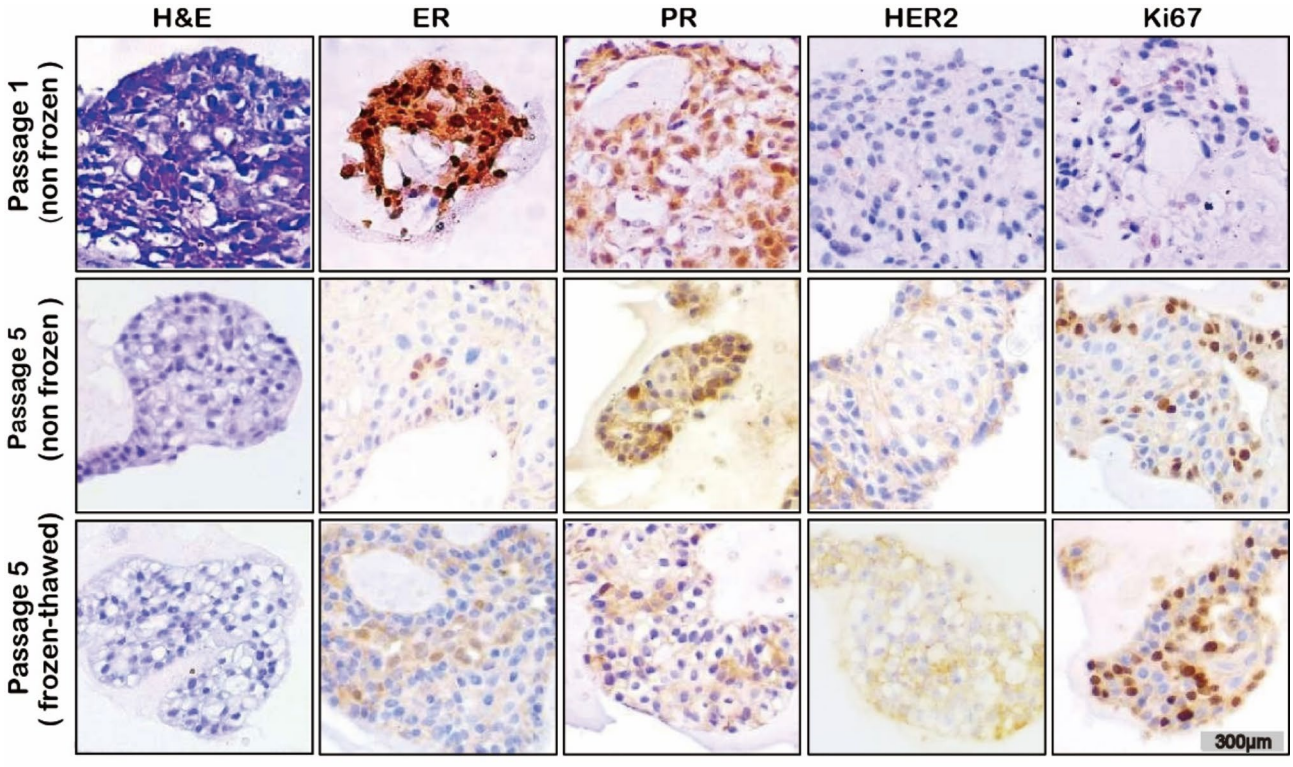

Fig. 3 The NETB patient-derived organoids exhibit stability. Representative images of H&E and immunohistochemistry staining (ER, PR, HER2, Ki67) of the NETB patient-derived organoids at passage 1 and passage 5, and after thawing at passage 5 are presented

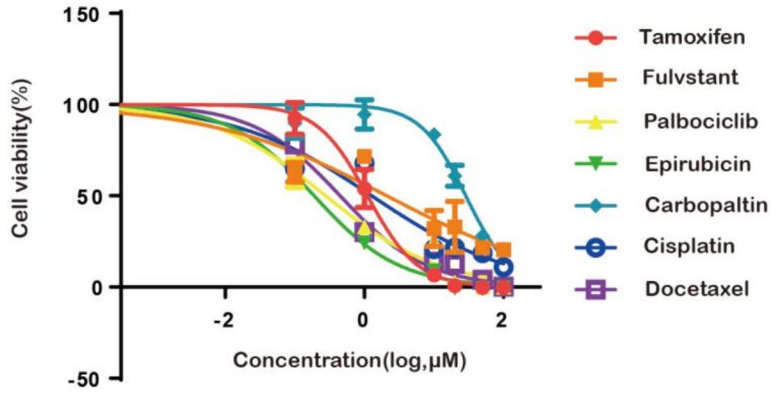

Medicine	IC50(μmol/L)
Tamoxifen	1.111
Fulvstant	2.104
Palbociclib	0.2786
Epirubicin	0.1900
Carbonpaltin	28.71
Cisplatin	1.27
Docetaxel	0.4487

Fig. 4 Drug sensitivity of the NETB patient-derived organoids. The x-axis represents drug concentration(log), the y-axis represents cell viability, and different colors represent different drugs. The organoids of fifth passage were treated, the duration of drug exposure was 5 days ($n=3$). The IC50 is the half-maximal inhibitory concentration for different drugs

different drugs, indicating an individualized response to each regimen.

Single-cell RNA sequencing revealed the presence of various cell subpopulations within the NETB patient-derived organoids

By clustering single-cell gene expression data, seventeen subgroups with different gene expression profiles were identified (Fig. 5A). These results demonstrated a degree of heterogeneity among the NETB patient-derived organoids. The Feature Plot showed significant differences in the expression of differential genes between the seventeen clusters, highlighting the reliability and stability of the clustering. To identify the main cell types in this atlas, each cluster was annotated based on marker gene expression. The cells were classified into three types: Basal cells (KRT14, KRT5, TP63, KRT17) [20, 21], Luminal epithelial cells (KRT18, KRT8, KRT19, FOXA1, MUC1) [22] and Proliferating basal cells (MKI67, TOP2A, KRT14, KRT5, TP63, KRT17) [23] (Fig. 5B and Supplement Table 1). The heatmap separately displayed the expression proportions and relative expression levels of marker genes in three clusters (Fig. 5C). Furthermore, we showed the expression of ESR1, ESR2, PGR, and ERBB2 (Fig. 5D).

To analyze the evolutionary dynamics of NETB patient-derived organoids, we also constructed a pseudotime trajectory analysis of the three cell clusters and generated a single-branch trajectory that depicted the tumor's development (Fig. 5E). All Basal cells (BASAL) were located at the starting point, while Luminal epithelial cells (Luminal_epi) were entirely positioned at the differentiated endpoint (Fig. 5F). Over the course of differentiation, changes in gene expression were observed, resulting in the clustering of cells into three distinct clusters based on their gene expression profiles (Fig. 5G). Over time, the expression of DKK3 and CDH3 gradually decreased. DKK3, an inhibitor of the WNT pathway, plays a crucial role in suppressing cancer cell proliferation and differentiation. Thus, its reduced expression could disrupt this function [24]. CDH3, a calcium-dependent cell adhesion protein, when decreased, could enhance the migration of cancer cells [25]. Subsequently, during this process, the expression of genes that promoted cancer cell proliferation, migration, and invasion gradually increased, including LIMCH1, MGLL, and PDK4 [13, 26, 27] (Fig. 5G).

GO enrichment analysis revealed significant enrichment in pathways related to cell migration and motility (Fig. 5H). Meanwhile, KEGG enrichment analysis revealed significant enrichment in various cancer related pathways, including PI3K-Akt signaling pathway, Rap1 signaling pathway, and MAPK signaling pathways (Fig. 5I). These suggested that the NETB patient-derived organoid culture effectively preserved the biological functions of NETB cells, providing a robust cell model and microenvironment for future research into the development and progression of NETB.

Protein-protein interaction network analysis identified CTNNB1, PTPN11, and ITGB1 as major core components (Fig. 5J). CTNNB1 encoded the β-catenin protein involved in the Wnt/β-catenin signaling pathway and is associated with the activity of estrogen and androgen receptors [28]. The PTPN11 gene is related with the proliferation of breast cancer cells [29]. ITGB1 is crucial in cell signaling pathways associated with resistance to chemotherapy in breast cancer [29]. Currently, there is limited research on this topic. These protein interactions may contribute to understanding the molecular mechanisms of NETB disease, and could offer potential value in its targeted treatment.

Discussions

In 1963, Feyrter and Hartmann firstly proposed that invasive breast carcinoma shares morphological similarities with colorectal cancer [30]. Subsequently, Cubilla described the growth patterns of 8 cases of breast carcinoid [31]. In 2003, the WHO officially recognized neuroendocrine neoplasms of the breast as a distinct subtype of breast cancer, suggesting that these tumors result from the differentiation of breast epithelial cells during carcinogenesis, rather than from pre-existing neuroendocrine stem cells [32]. Currently, the 5th edition of the WHO guidelines has further clarified the diagnostic criteria for NETB based on the histological and immunophenotypic characteristics of tumor cells [1]. Some scholars had conducted studies and discussions on the treatment of neuroendocrine neoplasms of the breast. Emily reported a case of the neuroendocrine neoplasm of the breast with Merkel cell features, which was extremely aggressive. At 5 weeks postoperatively, she presented with widely metastatic disease [33]. Some studies have explored tumor molecular markers. Nelli Roininen concluded that the prognostic factors of intestinal neuroendocrine tumor and NETB were quite similar. Additionally, it was speculated that treatment with somatostatin analogs might be effective for NETB due to the wide expression of SSTR-2 A [34]. There also was a clinical case report describing the dramatic response to cyclin D4/6 inhibitor in refractory, poorly differentiated NETB [35]. Several potential targets have also been proposed, including FOLR1, TROP-2, and H3K36Me3 [36, 37]. Based on a statistical analysis of the treatment outcomes for 22 NETB patients, it was recommended to perform radical surgery followed by postoperative radiotherapy [38].

Currently, there are no specific guidelines for the treatment of neuroendocrine neoplasms of the breast, either domestically or internationally. Clinically, treatments similar to those used for conventional breast cancer are often employed. In our previous studies, the breast

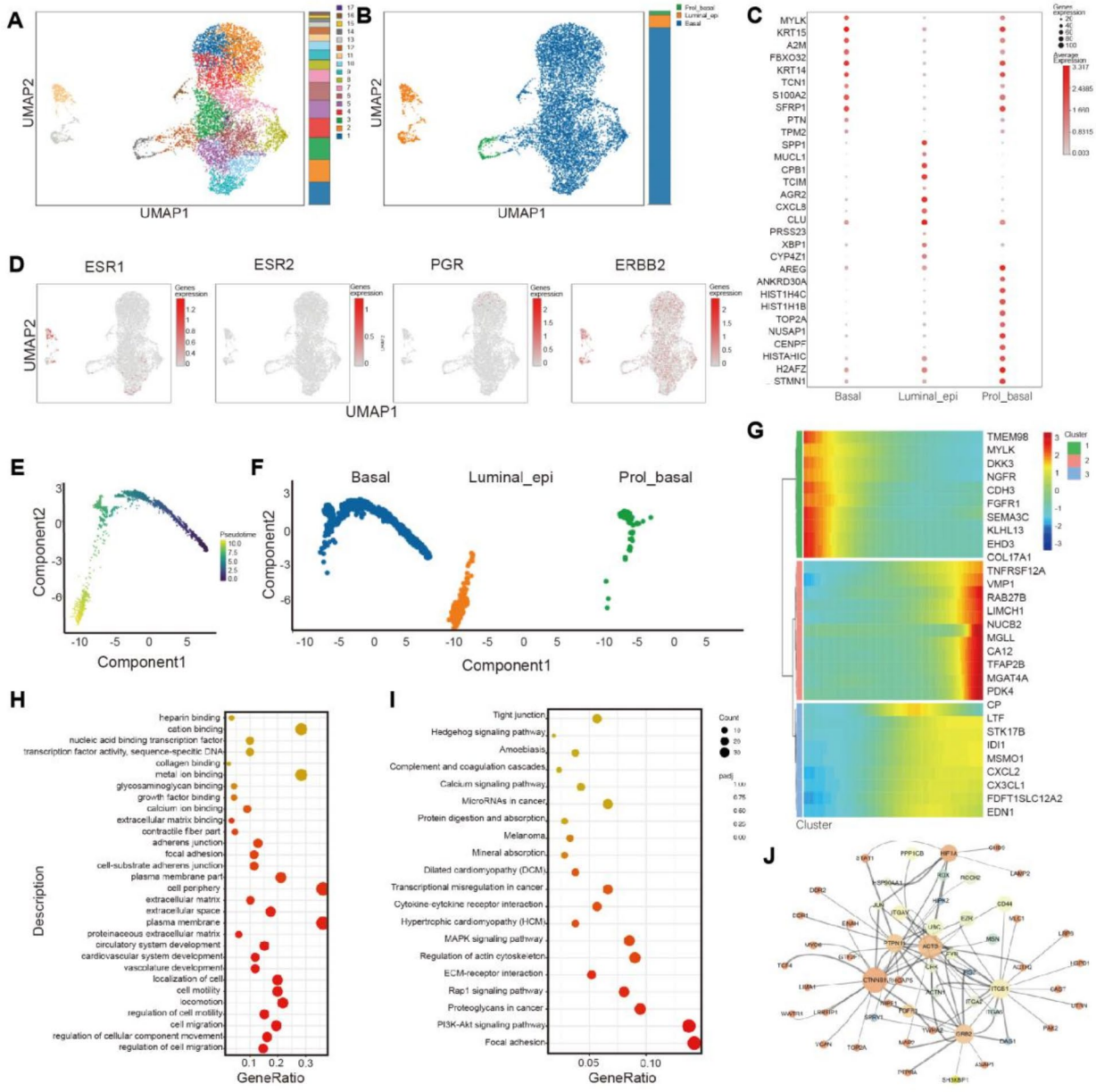

Fig. 5 Single-cell RNA-seq analysis of the NETB patient-derived organoids. **(A)** The t-SNE plot showing 17 clusters. The bar chart showing the proportion of each cluster. Each cluster was shown in a different color. **(B)** The t-SNE plot showing 3 cell types. The bar chart showing the proportion of each type. Each type was shown in a different color. **(C)** The heatmap separately displayed the expression proportions and relative expression levels of marker genes in three clusters. **(D)** The images of the ESR1, ESR2, PGR and ERBB2 expression. **(E)** The pseudotime trajectory analysis generated a single-branch trajectory that depicted the tumor's development. **(F)** Different cell types in the trajectory were marked with different colors. **(G)** Heatmap showing all cells along the pseudo-time, which was clustered into three profiles. Color key differentially coding from blue to red indicated the relative expression levels from low to high. **(H)** The GO enrichment dot plot showing enriched pathways on the vertical axis and the ratio of differentially expressed genes annotated to GO terms to the total number of differentially expressed genes on the horizontal axis. The size of the dots represents the number of genes, and the color gradient from red to blue indicates the level of enrichment significance, with red representing higher significance and blue lower significance. **(I)** The KEGG enrichment dot plot displayed enriched pathways on the vertical axis and the ratio of differentially expressed genes annotated to KEGG pathway IDs to the total number of differentially expressed genes on the horizontal axis. The size of the dots indicates the number of genes, while the color gradient from red to blue represents the enrichment significance, with red indicating higher significance and blue indicating lower significance. **(J)** The network structure diagram corresponding to the protein-protein interaction analysis

cancer patient-derived organoids were used as an ideal tool to mimic the tumor growth and drug responsiveness in vitro [14, 15]. In this study, we successfully established the NETB patient-derived organoids, which exhibited stability and maintained similar structure and molecular properties over more than 8 months (Supplement Fig. 1). We performed pathological experiments on the original tumor tissue and the NETB patient-derived organoids at different stages to confirm the histological features and molecular properties (Figs. 2 and 3). After eight months of incubation, the morphological differences were not significant. The organoids partly retained characteristics of the primary tumor, the expression of corresponding receptors, such as ER, gradually decreased after a long-term passage. Similar phenomena were reported previously [39, 40]. Additionally, the results showed the expression of Ki67 was enhanced compared to the primary tissue and increased with the passages. The similar phenomenon has been reported in other studies [41, 42]. Ki67 is commonly regarded as a proliferation marker associated with cell proliferation [43]. The culture media used to grow organoids is typically enriched with growth factors that promote cell proliferation. As the passage number increased, the fastest growing population of organoids was selected and gradually increased. However, ERBB2 expression is indeed a question worth exploring. Previous studies have reported that ERBB2-positive organoids exhibit higher expression levels than those found in primary breast cancer tissue [43]. The biological disparities observed between organoids and primary tumor tissues could be influenced by oxygen-enriched culture conditions. This suggests that we should strive to maintain the stability of organoid phenotypes by minimizing external environmental disturbances, including but not limited to oxygen levels. In conclusion, preserving hormone receptor expression at a high level is challenging due to the selective pressure of the external microenvironment. Improving long-term fidelity in organoids is a worthwhile pursuit in this field.

The NETB patient-derived organoids exhibited various sensitivities to the different drugs, indicating an individualized response to each regimen. Single-cell RNA sequencing revealed significant heterogeneity and diverse molecular functions among the NETB patient-derived organoids. Additionally, several genes and pathways associated with tumor proliferation and migration were identified, which may assist future targeted treatment for NETB (Fig. 5).

However, this study has several limitations. The first limitation is the small number of cases. Since NETB is relatively rare compared to common breast cancer types, obtaining sufficient samples has proven challenging. Additionally, we did not perform Single-cell RNA sequencing of the primary tumor tissue due to the limited size of tissues we could acquire. Lastly, although we observed some biological disparities between primary tumor and NETB patient-derived organoids, we did not design the experiment to explore the underlying reasons and mechanisms behind this phenomenon. In the future, we plan to conduct a long-term program to acquire more samples and design subsequent experiments to investigate this question.

Abbreviations

NETB	Neuroendocrine tumor of the breast
WHO	World Health Organization
3D	Three-dimensional
MRI	Magnetic Resonance Imaging
H&E	Hematoxylin and eosin
ER	Estrogen receptor
PR	Progesterone receptor
HER2	Human epidermal growth factor receptor 2
Syn	Synaptophysin
CgA	Chromogranin A
BASAL	Basal cells
Luminal_epi	Luminal epithelial cells
Prol_basal	Proliferating basal cells

Supplementary Information

The online version contains supplementary material available at https://doi.org/10.1186/s12935-024-03621-w.

Supplementary Material 1

Supplementary Material 2

Acknowledgements
Not applicable.

Author contributions
Dongyi Zhao was primarily responsible for all experimental procedures and contributed to manuscript writing and figure creation. Xue Bai and Shida Zhu wrote the manuscript, contributed to figure creation, and analyzed the Single-cell RNA sequencing data. Xuelu Li and Zuowei Zhao were mainly responsible for the supervision of the manuscript and the organization of ideas for the article. All authors read and approved this manuscript.

Funding
The financial assistance is provided by the National Natural Science Foundation of China (82203800, 82072934), Natural Science Foundation of Liaoning Province (2023-MSLH-022, JG24DB110), and 1 + X program of the Second Hospital of Dalian Medical University (2022LCYJYB03, 2022QNJXJYFH01, 2022JXGGYJ011).

Data availability
The data discussed in this publication have been deposited in NCBI's Gene Expression Omnibus (Edgar et al., 2002) and are accessible through GEO Series accession number GSE284118 (https://www.ncbi.nlm.nih.gov/geo/query/acc.cgi?acc=GSE284118).

Declarations

Ethics approval and consent to participate
Tumor specimens were obtained with the approval of the ethics committee of The Second Hospital of Dalian Medical University. Written informed consent was obtained from the patient.

AI disclosure
Not applicable.

Consent for publication
Not applicable.

Competing interests
The authors declare no competing interests.

Received: 26 August 2024 / Accepted: 14 December 2024
Published online: 27 December 2024

References

1. Board W. C.o.T.E. WHO classification of tumors. 5th Edition. Breast tumours. *Lyon, France: IARC* (2019).
2. Vegni F, et al. Neuroendocrine neoplasms of the breast: a review of literature. Virchows Arch. 2024;485:197–212.
3. Ozsen M, Senol K, Tolunay S, Gokgoz MS, Evrensel T. Histopathological features Predicting Neuroendocrine morphology in primary breast tumors: a retrospective analysis. Eur J Breast Health. 2024;20:110–6.
4. Kinoshita S, et al. Primary small-cell neuroendocrine carcinoma of the breast: report of a case. Surg Today. 2008;38:734–8.
5. Irelli A et al. Neuroendocrine Cancer of the breast: a rare entity. J Clin Med 9(2020).
6. Ji S, et al. A case of primary large-cell neuroendocrine carcinoma of the breast. Asian J Surg. 2024;47:3254–5.
7. Rosen LE, Gattuso P. Neuroendocrine tumors of the breast. Arch Pathol Lab Med. 2017;141:1577–81.
8. Mohamed A, Zeidalkilani J, Asa SL, Trybula M, Montero AJ. Management of neuroendocrine breast carcinoma (NEBC): review of literature. Oncol Rev. 2024;18:12114.
9. Sachs N, et al. A living biobank of breast Cancer Organoids captures Disease Heterogeneity. Cell. 2018;172:373–e386310.
10. Dekkers JF, et al. Long-term culture, genetic manipulation and xenotransplantation of human normal and breast cancer organoids. Nat Protoc. 2021;16:1936–65.
11. Guillen KP, et al. A human breast cancer-derived xenograft and organoid platform for drug discovery and precision oncology. Nat Cancer. 2022;3:232–50.
12. Lin CJ, et al. Genetic interactions reveal distinct biological and therapeutic implications in breast cancer. Cancer Cell. 2024;42:701–e719712.
13. Kong LR et al., *A glycolytic metabolite bypasses two-hit tumor suppression by BRCA2. Cell 187, 2269–2287.e2216 (2024).*
14. Li X, et al. Breast cancer organoids from a patient with giant papillary carcinoma as a high-fidelity model. Cancer Cell Int. 2020;20:86.
15. Pan B, et al. Establishment and characterization of breast cancer organoids from a patient with mammary Paget's disease. Cancer Cell Int. 2020;20:365.
16. Wolf FA, Angerer P, Theis FJ. SCANPY: large-scale single-cell gene expression data analysis. Genome Biol. 2018;19:15.
17. Qiu X, et al. Single-cell mRNA quantification and differential analysis with Census. Nat Methods. 2017;14:309–15.
18. Yu G, Wang LG, Han Y, He QY. clusterProfiler: an R package for comparing biological themes among gene clusters. Omics. 2012;16:284–7.
19. Szklarczyk D, et al. The STRING database in 2023: protein-protein association networks and functional enrichment analyses for any sequenced genome of interest. Nucleic Acids Res. 2023;51:D638–46.
20. Nguyen QH, et al. Profiling human breast epithelial cells using single cell RNA sequencing identifies cell diversity. Nat Commun. 2018;9:2028.
21. Liu SQ, et al. Single-cell and spatially resolved analysis uncovers cell heterogeneity of breast cancer. J Hematol Oncol. 2022;15:19.
22. Kumar T et al. A spatially resolved single cell genomic atlas of the adult human breast. bioRxiv (2023).
23. Wu SZ, et al. A single-cell and spatially resolved atlas of human breast cancers. Nat Genet. 2021;53:1334–47.
24. Yao J et al. lnc–MICAL2–1 sponges miR–25 to regulate DKK3 expression and inhibits activation of the Wnt/β–catenin signaling pathway in breast cancer. Int J Mol Med 49(2022).
25. Hwang PY, et al. A Cdh3-β-catenin-laminin signaling axis in a subset of breast tumor leader cells control leader cell polarization and directional collective migration. Dev Cell. 2023;58:34–e5039.
26. Xiang W, et al. Monoacylglycerol lipase regulates cannabinoid receptor 2-dependent macrophage activation and cancer progression. Nat Commun. 2018;9:2574.
27. Dou X, et al. PDK4-dependent hypercatabolism and lactate production of senescent cells promotes cancer malignancy. Nat Metab. 2023;5:1887–910.
28. Ozcan G. PTCH1 and CTNNB1 emerge as pivotal predictors of resistance to neoadjuvant chemotherapy in ER+/HER2- breast cancer. Front Oncol. 2023;13:1216438.
29. Wang LB, et al. Proteogenomic and metabolomic characterization of human glioblastoma. Cancer Cell. 2021;39:509–e528520.
30. Feyrter F, Hartmann G, [ON, The carcinoid growth form of the carcinoma mammae. Especially the carcinoma solidum (Gelatinosum) Mammae]. Frankf Z Pathol. 1963;73:24–39.
31. Fisher ER, Palekar AS. Solid and mucinous varieties of so-called mammary carcinoid tumors. Am J Clin Pathol. 1979;72:909–16.
32. Cloyd JM, et al. Impact of histological subtype on long-term outcomes of neuroendocrine carcinoma of the breast. Breast Cancer Res Treat. 2014;148:637–44.
33. Albright EL, Keeney ME, Bashir A, Weigel RJ. Poorly differentiated neuroendocrine carcinoma of the breast with Merkel cell features. Breast J. 2018;24:644–7.
34. Ang D, et al. Novel mutations in neuroendocrine carcinoma of the breast: possible therapeutic targets. Appl Immunohistochem Mol Morphol. 2015;23:97–103.
35. Shanks A, Choi J, Karur V. Dramatic response to cyclin D-dependent kinase 4/6 inhibitor in refractory poorly differentiated neuroendocrine carcinoma of the breast. Proc (Bayl Univ Med Cent). 2018;31:352–4.
36. Patel G, Bipte S. Updates in primary neuroendocrine breast carcinoma - a case report and review of literature. J Cancer Res Ther. 2020;16:1528–31.
37. Zouki DN, et al. CDK4/6 and aromatase inhibitors as first-line treatment in metastatic high-grade neuroendocrine carcinoma of the breast: a case report. Clin Case Rep. 2024;12:e9180.
38. Püsküllüoğlu M, et al. Non-metastatic primary neuroendocrine neoplasms of the breast: a reference cancer center's experience of a heterogenous entity. Front Endocrinol (Lausanne). 2024;15:1217495.
39. Campaner E et al. Breast Cancer Organoids Model patient-specific response to Drug Treatment. Cancers (Basel) 12(2020).
40. Rosenbluth JM, et al. Organoid cultures from normal and cancer-prone human breast tissues preserve complex epithelial lineages. Nat Commun. 2020;11:1711.
41. Nagel S, et al. Multipotent nestin-positive stem cells reside in the stroma of human eccrine and apocrine sweat glands and can be propagated robustly *in vitro*. PLoS ONE. 2013;8:e78365.
42. Tong Y, Ueyama-Toba Y, Mizuguchi H. Biliary epithelial cell differentiation of bipotent human liver-derived organoids by 2D and 3D culture. Biochem Biophys Rep. 2023;33:101432.
43. Cuylen S, et al. Ki-67 acts as a biological surfactant to disperse mitotic chromosomes. Nature. 2016;535:308–12.

Publisher's note